SPECIAL SECTION PAPER

WILEY

Doubling the optical efficiency of color-converted micro-light-emitting diode displays with a patterned cholesteric liquid crystal polymer film

En-Lin Hsiang, SID Student Member[1] | Yannanqi Li, SID Student Member[1] |
Ziqian He, SID Student Member[1] | Tao Zhan, SID Student Member[1] |
Caicai Zhang, SID Student Member[2,3] | Yi-Fen Lan[4] |
Yajie Dong, SID Member[1,2,3] | Shin-Tson Wu, SID Fellow[1]

[1]College of Optics and Photonics, University of Central Florida, Orlando, Florida, USA

[2]Department of Materials Science and Engineering, University of Central Florida, Orlando, Florida, USA

[3]NanoScience Technology Center, University of Central Florida, Orlando, Florida, USA

[4]AU Optronics Corp., Hsinchu Science Park, Hsinchu, Taiwan

Correspondence
Shin-Tson Wu, College of Optics and Photonics, University of Central Florida, Orlando, FL 32816, USA.
Email: swu@creol.ucf.edu

Funding information
a.u.Vista, Inc.

Abstract

We propose a patterned cholesteric liquid crystal (CLC) polymer film as a self-assembled Bragg reflector to enhance the performance of a color-converted micro-light-emitting diode (LED) display system. In the display system, we firstly optimize the device structure of blue LED chip to maintain a high light extraction efficiency and low optical crosstalk. Next, we fabricate several patterned CLC films with feature sizes ranging from 10 to 80 μm. By integrating the patterned CLC film into a color-conversion micro-LED display, the optical efficiency is doubled while keeping a color gamut of about 90% Rec. 2020. Finally, we carry out a proof-of-concept experiment to validate the functionality of such a patterned CLC film.

KEYWORDS

cholesteric liquid crystal, color-conversion efficiency, micro-LED display, perovskite nanocrystals

1 | INTRODUCTION

Micro-light-emitting diode (LED) is emerging as a potentially disruptive display technology.[1,2] To obtain vivid colors, a blue micro-LED array overcoated with quantum dot (or perovskite nanocrystal) color filters (QDCFs) prepared by inkjet printing or photolithography are widely used.[3–5] However, several problems remain to be overcome, such as blue light leakage, low color-conversion efficiency (CCE), and optical crosstalk. A conventional method to prevent the blue light leakage is to laminate another pigment color filter (CF) array on top of it. As Gou et al. demonstrated,[6] the CF array not only absorbs the leaked blue light but also prevents ambient light excitation. However, the absorbed blue light is wasted. In order to improve the CCE of the QD film, it has been proposed to deposit a distributed Bragg reflector (DBR) on top of the QD film.[7,8] Generally, at least five pairs of TiO_2/SiO_2 should be used in DBR to obtain an adequate reflectivity in the blue spectral region, while maintaining high transmittance to the green and red channels. The leaked blue light will be recycled by the DBR to re-enter and excite the color-conversion material. As a result, a higher CCE and a wider color gamut can be obtained. However, if we consider the RGB (red, green, and blue) subpixels together, we should pattern the DBR layer to cover only the red and green subpixel areas and avoid blocking the blue subpixels. Due to the high cost and complicated fabrication process of the patterned DBR, there is still a lack of commercial products.

Cholesteric liquid crystal (CLC) polymer film is another method to form self-assembled Bragg reflectors through a low-cost, simple fabricating process.[9] However, the display performance of the color-conversion micro-LED display integrated with the CLC film is still lacking. In this article, we propose a patterned CLC polymer film to improve the performance of color-converted micro-LED displays. The proposed patterned CLC film consists of two textures: focal-conic texture (FC-CLC) and planar texture (P-CLC). The P-CLC covering the red and green subpixels is used as a DBR to recycle the leaked blue light. Meanwhile, because the CLC film is thin, the FC-CLC maintains high transmittance to the blue subpixel. Here, we have fabricated several patterned CLC films with sizes ranging from 10 to 80 μm and measured their optical properties for further optimization. In addition, a hybrid QDCF, which consists of cadmium (Cd)-based red QD and homemade green perovskite nanocrystals is applied as a color-conversion film to widen the color gamut.[10] According to our simulation results, the patterned CLC film with optimized reflection band can restore the leaked blue light and reduce the crosstalk between the blue and green CFs. Therefore, our patterned CLC polymer film can boost the CCE of the display system by approximately two times. Finally, we conduct a proof-of-concept experiment to verify the function of such a patterned CLC film.

2 | DEVICE STRUCTURE

2.1 | Color-converted micro-LED display

Figure 1 shows the device structure of the proposed color-converted micro-LED display. It consists of a blue micro-LED array at the bottom, an adhesion layer, a patterned color-conversion film, a patterned CLC film, and a top CF array to form RGB subpixels. The blue LED array is protected and planarized by black photoresist to prevent lateral leakage of blue light.[11,12] The blue light emitted from the top passes through the adhesion layer and is down converted into green and red lights by the QD or perovskite material. Afterward, the leaked blue light is recycled by the patterned CLC to improve CCE. Here, a CLC film with opposite handedness is assembled to recover the unpolarized leakage light from blue micro-LED. Finally, the CFs are aligned with the RGB subpixels to absorb the rest blue light and prevent ambient light excitation. To evaluate the improvement resulting from adding a patterned CLC film to the display system, the device performance without such a CLC film is also analyzed below. In the following, we set the subpixel size as 100 μm × 200 μm and the LED chip size as 50 μm × 100 μm. To analyze the severity of optical crosstalk, the employed adhesion layer is in the 20 to 60 μm range.

We use ray tracing software (LightTools) to simulate the performance of our proposed display system. The emission spectrum of the blue LED is shown in Figure 2A, and its optical performance will be analyzed later. The photoluminescence characteristics of QD are simulated by Advanced Physics Module in LightTools. The absorption and emission spectra of green perovskite nanocrystals and cadmium-based red QDs are also plotted in Figure 2A.[13,14] In our model, the mean free path is the average length of ray propagation before impacting QD particles, which is used to express the concentration of the color-conversion film. Due to the photolithographic fabrication process,[15] the color-conversion film thickness is limited to 5–9 μm. A thicker QD film would reduce the blue light leakage, but the self-absorption effect is also more pronounced. The photoluminescence quantum yield (PLQY) of our perovskite film[13] is 0.7, and the refractive index of the color-conversion film is 1.5. In addition, two types of CFs are used in our simulation, and their transmission spectra are shown in Figure 2B. Compared with CF1, CF2 provides a wider color gamut but at the expense of lower optical efficiency.

2.2 | Patterned CLC polymer film

The fabrication process of patterned CLC film is illustrated in Figure 3. In experiment, we prepared a CLC precursor consisting of 92.95 wt.% reactive mesogen RM257 (from HCCH) as LC monomer, 2.8 wt.% S5011 or R5011
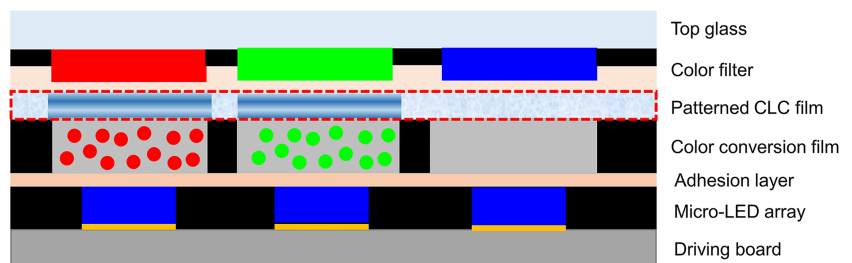

FIGURE 1 Device configuration of the proposed color-converted micro-light-emitting diode (LED) display

Top glass
Color filter
Patterned CLC film
Color conversion film
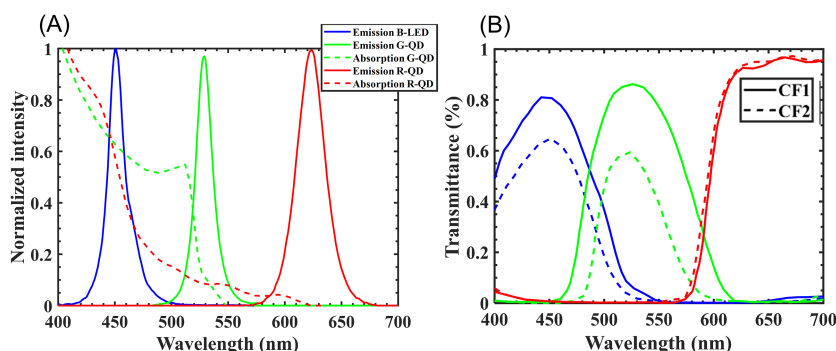Adhesion layer
Micro-LED array
Driving board

FIGURE 2 (A) Emission spectrum of the blue micro-light-emitting diode (LED); absorbance (dashed lines) and photoluminescence spectra of green perovskite nanocrystal and red quantum dot (QD). (B) Transmission spectra of color filters CF1 and CF2
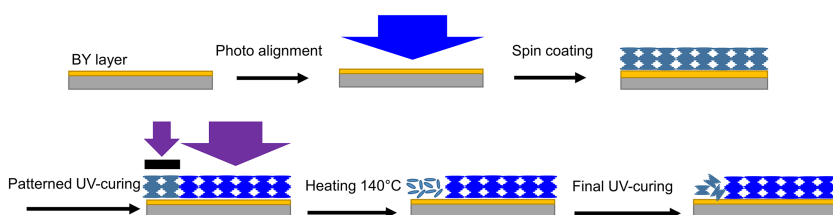

FIGURE 3 Fabrication process of the proposed patterned cholesteric liquid crystal (CLC) film
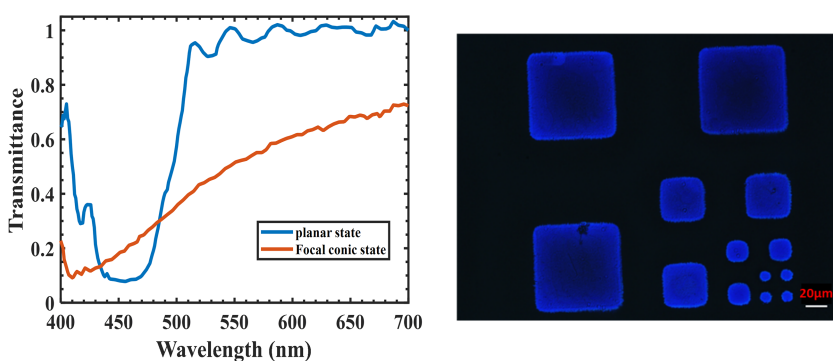

FIGURE 4 (A) Measured transmission spectra of the planar state and the focal-conic texture on a patterned cholesteric liquid crystal (CLC) film. (B) Microscope images showing a patterned CLC film with 10-, 20-, 40-, and 80-μm feature sizes

chiral dopants (from HCCH), 4 wt.% of photoinitiator Irgacure 651 (from BASF), and 0.25 wt.% of surfactant Zonyl 8857A (from DuPont). First, we spin coated a thin Brilliant Yellow (BY) photoalignment layer on a clean glass substrate and then illuminated it by a blue laser ($\lambda = 450$ nm) to create the alignment pattern. Next, we spin coated the CLC precursor on top of the BY layer to replicate the alignment. In our design, in order to reflect blue light, the helical pitch length of the CLC is set at ~298 nm and the film thickness is about eight helical pitches to establish Bragg reflection. Then, we conducted the patterned UV curing process to create two different textures on the CLC film. The photopolymerization process was only carried out in the transparent area to form a stable polymer film (P-CLC). After that, the sample was heated to 140°C, and the CLC material in the unexposed area (FC-CLC) became isotropic. Last, the cooling process and UV curing were performed simultaneously. During the cooling process, the LC changed from isotropic back to cholesteric, and the arrangement was completely random.

Figure 4A depicts the transmission spectrum of the film's planar texture and focal-conic texture measured by a circularly polarized light having the same chirality as the CLC film. In addition, several kinds of patterned CLC films with different feature sizes were produced to prove that they can meet different display applications. Figure 4B shows some photomicrographs of patterned CLC films with feature sizes of 10, 20, 40, and 80 μm.

In addition, we also simulated the optical performance of the patterned CLC films[16] fabricated using a high birefringence (Δn) LC monomer (e.g., Merck RMS16/091, $\Delta n = 0.3$ at $\lambda = 450$ nm). Such a high Δn material helps to broaden the reflection band of the P-CLC film. Here, we name the film made with $\Delta n = 0.3$ as the wide-band (WB) CLC film and the film made with RM257 LC monomer as the narrow-band (NB) CLC film.

The average reflectance of the P-CLC film in the blue spectral region can be calculated by the following formula:

$$R_\theta = \frac{\int S_{LED}(\lambda) \times R_{CLC}(\lambda,\theta)d\lambda}{\int S_{LED}(\lambda)d\lambda}, \qquad (1)$$

where S_{LED} is the spectral power density of blue light emitted by the micro-LED and R_{CLC} is the reflection spectra of CLC film at different incident angles.

Based on Equation 1, the average reflectivity of the WB and NB CLC films as a function of incident angles is plotted in Figure 5A. On the other hand, in the FC-CLC segment, the tiny multidomain CLCs with random distribution scatter the incident light. The total transmittance is about 95%, and its angular transmission profile is plotted in Figure 5B. Unlike the reflection band of P-CLC, which exhibits a strong polarization selectivity, the scattering property of FC-CLC is polarization independent. The measured optical properties of the patterned CLC film will be further applied in our LightTools model to evaluate the display performance of color-converted micro-LED display integrated with the CLC film.

2.3 | Blue micro-LED array

The device structure of the thin-film flip-chip LED is shown in Figure 6A. It consists of a metal mirror with high reflectivity, a p-GaN layer (about hundreds of nanometers), a multiple quantum well (MQWs) layer (about 100 nm), and an n-GaN layer (about a few microns). For the emission source, due to the valence band characteristics of GaN, anisotropic InGaN emission with the dipole axis parallel to the crystal C plane (only in-plane dipole) is considered.[17] The light intensity of the TM component is much smaller than that of the TE component.[18] The

FIGURE 5 (A) Average reflectivity of wide-band (WB) and narrow-band (NB) planar cholesteric liquid crystal (P-CLC) films in the blue light spectrum (micro-light-emitting diode [LED]) at different incident angles (in air). (B) Measured angular transmission profile of the focal-conic CLC film at normal incidence
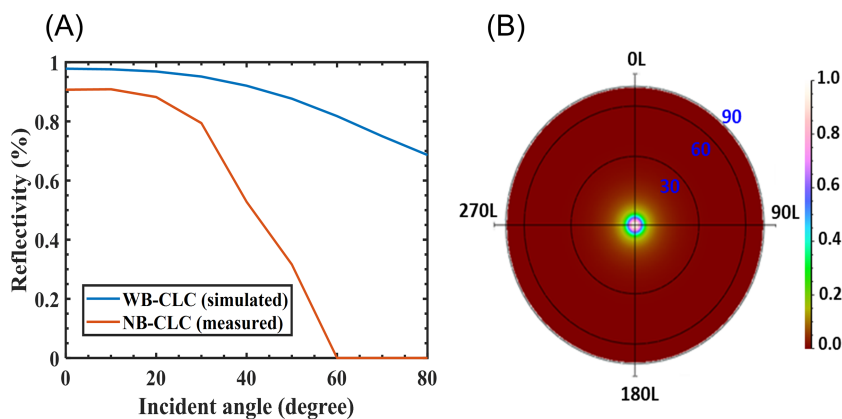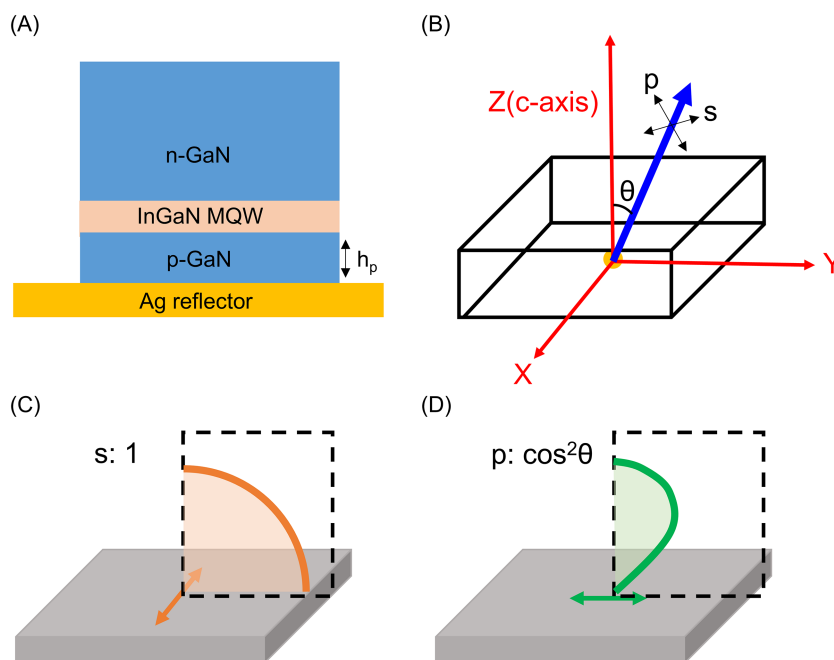

FIGURE 6 (A) Schematic design of micro-light-emitting diode (LED) chips considered in this study. (B) Schematic diagrams of coordinate system in simulation and measurement. The angular distributions of (C) s-polarized component and (D) $\cos^2\theta$ of the p-polarized component

direction of light emission and the polarization vector can be represented by the azimuthal angle φ and the polar angle θ shown in Figure 6B. The electric field of p is in the same plane as the c axis and the direction of emitting ray. On the other hand, the electric field of s oscillates vertically to this plane and the electric field of p. The main TE component produces a light source consisting of s-polarized component and $\cos^2\theta$ of the p-polarized component, as shown in Figure 6C,D.[19]

Because the emitted MQW layer is close to the bottom mirror, the interference between the dipole source and the reflected light from the bottom mirror will form a high and low intensity area. The radiation pattern inside the LED chip varies with the thickness of the p-GaN layer. Here, the radiation pattern is simulated by the finite-difference time-domain (FDTD) method and the theoretical interference numerical equation. In both methods, the half-cavity approximation is applied.[20] The refractive index of GaN is 2.45, and Ag is 0.14 + 2.47i, so the reflectivity between p-GaN and Ag is about 90%.

Based on the interference theory, the radiation pattern can be described as

$$|E_{\text{total}}|^2 = E_0{}^2 + E_r{}^2 + 2E_0E_r \cos(\Phi_1 + \Phi_2),$$

where E_0 is the amplitude of the emitted light, E_r is the amplitude of the reflected light, Φ_1 is the phase shift due to optical path difference, and Φ_2 is the phase shift resulting from mirror reflection.

According to the light polarization (s or p polarization) and the material's refractive index, the phase shift at a specular reflection can be calculated by the Fresnel reflection theory. On the other hand, the phase shift caused by the optical path difference can be obtained by the following formula:

$$\Phi_1 = 2\pi \times \frac{\left(2 \times h_p \times \cos(\theta)\right)}{\lambda_n},$$

where h_p is the thickness of p-GaN, θ is the polar angle, and λ_n is the effective wavelength.

For the FDTD method, the simulated LED structure is shown in Figure 7A. Two dipoles aligned along x and y axes, corresponding to the s and p polarizations are simulated, respectively. In Figure 7B, the radiation pattern of p-GaN with a thickness of 100 nm simulated by the FDTD model is shown as dotted lines, and the radiation pattern calculated by the theoretical interference equation is drawn with a solid line. The agreement between these two methods is very good. In the following paragraph, the influence of p-GaN thickness on optical crosstalk will be analyzed.

3 | SIMULATION RESULTS AND DISCUSSIONS

3.1 | Optical crosstalk

Based on the above methods, we analyzed the radiation patterns of thin-film flip-chip LEDs with various p-GaN thicknesses (175, 200, 210, 225, 250, and 275 nm), and results are shown in Figure 8. Then, the angular distribution is imported into the ray tracing model in Monte Carlo LightTools to analyze the light extraction efficiency (LEE) of the blue LED array. Because the LED chip is surrounded by a black photoresist with a refractive index of 1.5, the light extraction cone ($\pm 38°$) is limited to the top surface of the LED. Figure 8 illustrates that with various thickness of p-GaN layer, the radiation pattern and LEE is changed periodically. The relatively high LEE region ($\geq 30\%$) occurs when the p-GaN thickness is at 210, 225, and 250 nm.

In addition to efficiency, optical crosstalk[6] that could reduce the image quality is another key factor for micro-LED color-conversion displays. Therefore, it is important to apply an appropriate thickness of p-GaN to achieve high LEE and small optical crosstalk. The angular distribution of the blue LED light incident on the color-conversion film depends on the radiation pattern inside the LED and the light extraction cone at the interface between the LED and the resin. For example, when the thickness of p-GaN is 250 nm, the radiation pattern
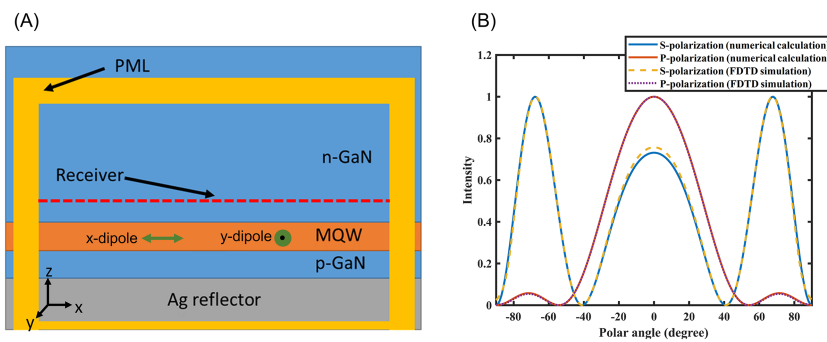

FIGURE 7 (A) Schematic diagram of the simulated light-emitting diode (LED) structure in FDTD simulation (half-cavity approximation is applied). (B) Simulated angular distribution inside the GaN LED by the FDTD model and by the interference theory ($h_p = 100$ nm)
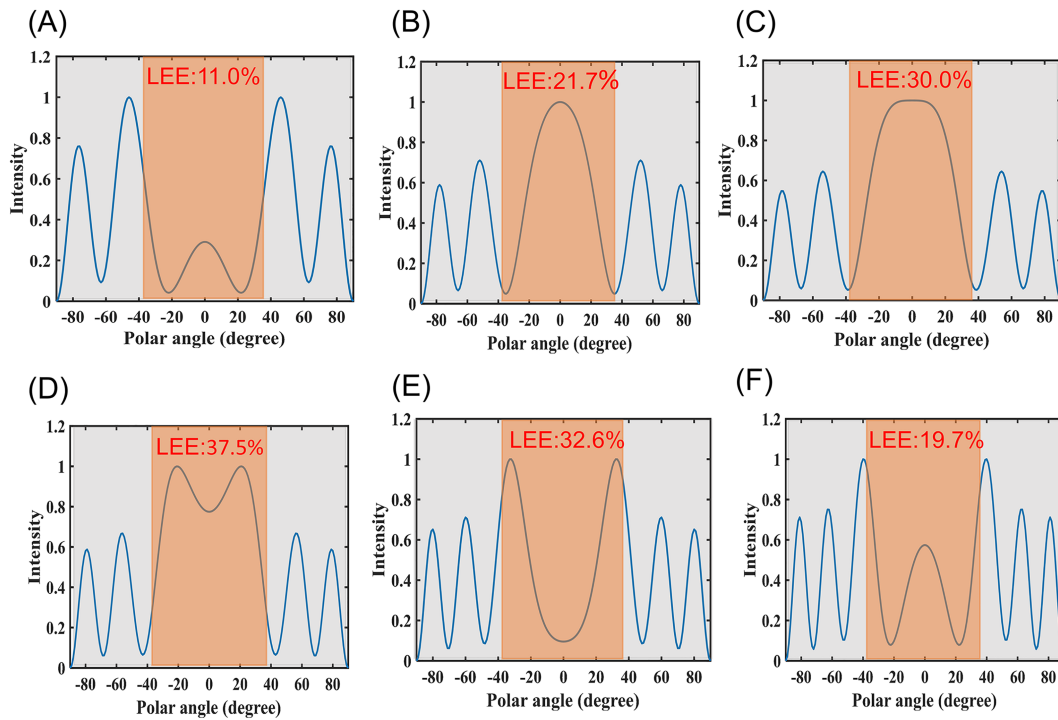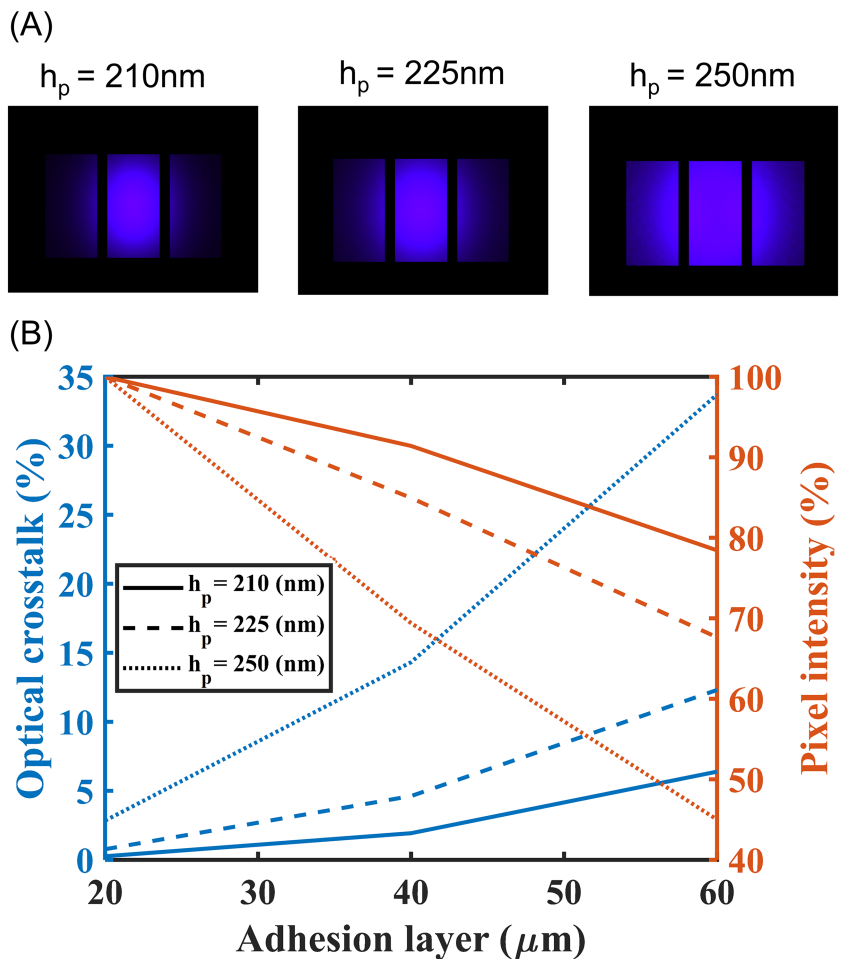
FIGURE 8 The angular distribution inside the GaN light-emitting diode (LED) by the interference theory (A) h_p = 175 nm, (B) h_p = 200 nm, (C) h_p = 210 nm, (D) h_p = 225 nm, (E) h_p = 250 nm, and (F) h_p = 275 nm

FIGURE 9 (A) Simulated color image at the top of adhesion layer (20 μm). (B) Simulated optical crosstalk ratio as a function of adhesion layer thickness

inside the LED has a peak intensity near the critical angle. Therefore, after the emitted light is refracted at the interface between the LED and the resin, the angular distribution inside the resin will have a strong intensity in large angle, which will cause severe optical crosstalk. Based on the device structure shown in Figure 1, when the adhesion layer is 20 μm, Figure 9 shows the optical crosstalk of micro-LED color-conversion displays with various p-GaN thicknesses (210, 225, and 250 nm). To assess how much blue light passing through adjacent pixels, we place the receiver on top of the adhesive layer (at the entrance of color-conversion material). From Figure 9A, we can see that when the p-GaN thickness is 210 nm, the smallest optical crosstalk occurs. In addition, a thicker adhesion layer also increases the optical crosstalk. Figure 9B shows the optical crosstalk ratio[6] as a function of adhesion layer thickness. Three micro-LEDs with p-GaN thickness (210, 225, and 250 nm) are analyzed. Taking the relatively large LEE (30.0%) and small optical crosstalk into consideration, the 210-nm p-GaN thickness micro-LED is used in the following analysis.

3.2 | CCE and color gamut

In this section, we evaluate the improvement in CCE and color gamut of our proposed patterned CLC film system relative to the control system. Four types of display systems are analyzed: (1) CF1 only (control system), (2) CF2 only (lower efficiency but wider color gamut), (3) CF1 + CLC film (NB), and (4) CF1 + CLC film (WB). As described above, the P-CLC film can reflect the leaked blue light back to the color-conversion film, thereby increasing CCE. Generally, the more blue light leaks, the greater the improvement of the P-CLC film. Therefore, it is important to make the blue light leakage rate close to the practical value. Based on Hu et al.[21] and Yue,[22] we found that the blue light leakage rate of most QDCFs is ~20% to 40%. In our simulation model, we use these numbers to analyze the CCE enhancement caused by the patterned CLC film. Figure 10 depicts the spectral power distribution and display color gamut of four types of display systems when the blue light leakage rate is 40%. We first focus on the comparison of CCE between different display systems. As described above, CF2, which has a lower transmittance than CF1, reduces the CCE. In addition, for display systems with P-CLC films, NB and WB CLC films lead to a CCE improvement of approximately 16% and 30%, respectively. Compared with the NB CLC film, as shown in Figure 5A, the WB CLC film with a larger reflection band has better blue light recycling ability.

In terms of color performance, the narrower emission spectra of green perovskite nanocrystals and red QD materials are expected to provide a wider color gamut. However, due to the blue light leakage in the blue-green crosstalk area of CF1, the display color gamut is reduced to 77% of Rec. 2020. To solve this problem, a CF (CF2) with less crosstalk between the blue and green channels can be applied to expand the color gamut. Compared with CF1, CF2 can expand the color gamut from 77% to 92% Rec. 2020. However, the average transmittance of CF2 in the emission spectrum of perovskite nanocrystals

TABLE 1 Summary of normalized color-conversion efficiency and color coverage of the four display systems studied

	Intensity (color converted)	Color coverage (Rec. 2020)
CF1	77%	77.46%
CF2	50%	92.70%
CF1 + NB CLC	89%	83.22%
CF1 + WB CLC	100%	89.50%

Abbreviations: CF, color filter; CLC, cholesteric liquid crystal; NB, narrow band; WB, wide band.
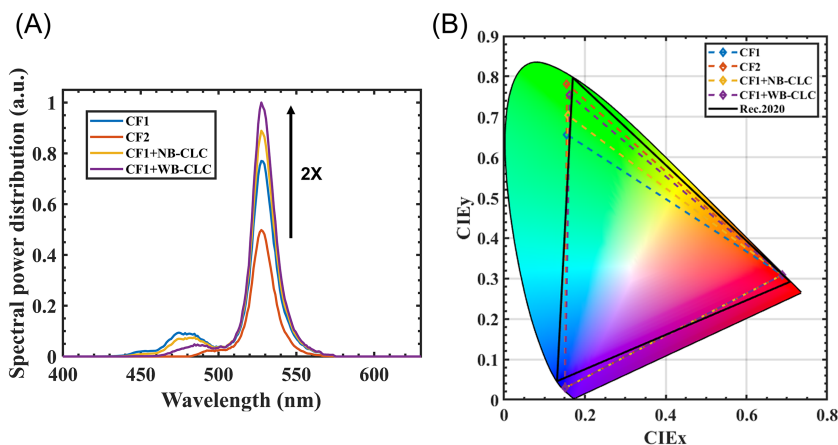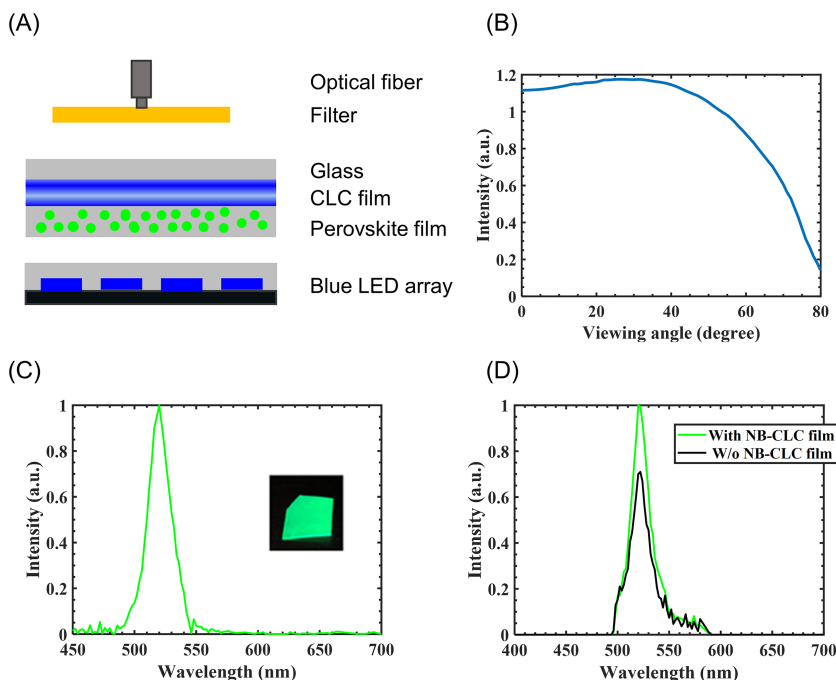

FIGURE 10 (A) Comparison of the spectral power distribution of the four specified display systems. (B) Simulated color gamut of the four display systems in Rec. 2020 color space

FIGURE 11 (A) Schematic diagram of the experimental setup. (B) Measured radiation pattern of the light-emitting diode (LED) array. (C) Measured emission spectrum of the CsPbBr3 perovskite film. Inset: CsPbBr3 perovskite film under 365-nm UV light. (D) Measured emission spectrum of down-converted green light with and without the cholesteric liquid crystal (CLC) film (filtered by the long pass filter with 500-nm cutoff wavelength)

is only 54.5%. Such a low transmittance greatly reduces the CCE of the display system. On the other hand, the WB CLC film has a wider reflection band (410–490 nm), which helps not only recycle the leaked blue light but also reduce the crosstalk between the green and blue CFs. Thus, the color gamut coverage is expanded. In addition, the WB CLC film can maintain high transmittance in the emission spectrum of the perovskite nanocrystals. As a result, by combining a high-transmittance CF (CF1) with a WB CLC film, a wide color gamut (89.5% Rec. 2020) and high CCE can be achieved simultaneously. In comparison with CF2, our newly proposed device structure can achieve a similar color gamut (around 90% Rec. 2020) but with a twice CCE. Table 1 summarizes the overall CCE and color coverage of the four types of display systems.

4 | PROOF-OF-CONCEPT EXPERIMENT

Figure 11A illustrates the setup of our proof-of-concept experiment. In order to recycle the leaked blue light, two CLC films with opposite handedness are laminated on top of a CsPbBr3-polystyrene perovskite-polymer. Due to the limitations of our manufacturing equipment, in this experiment, the micro-LED array is replaced by an LED array. However, there are some differences between these two device structures. For example, the backward reflector at the bottom of the micro-LED and the black photoresist to prevent lateral emission is not applied in

the LED array. The radiation pattern of the LED array was measured by a goniometer (RiGO801 TechnoTeam Vision) and plotted in Figure 11B. In addition, as shown in Figure 11C, a CsPbBr3-polystyrene perovskite-polymer composite film with a center wavelength of 520 nm and a full width at half maximum (FWHM) of 21 nm was prepared by the swelling microencapsulation method.[23] A control measurement based on a glass substrate was also prepared to evaluate the effectiveness of the CLC film, and the blue light leakage rate of display system without CLC film was measured to be 60%. Comparing the normalized emission spectra received by the fiber-optic spectrometer (Ocean Optics HR2000CG-UV-NIR) drawn in Figure 11D from the device structure with and without the CLC film, the CLC film improves the CCE of the color-conversion film by about 43% (under 60% blue light leakage). In the measurement, a long pass filter (cutoff wavelength of 500 nm) was used as a CF. It is worth noting that although the optical fiber can only receive the light emitted near the normal angle, according to the isotropic emission of the perovskite nanocrystal, the intensity increase ratio should be the same at all angles.

Here, we only compared the results of the display system with and without NB CLC film. The reflection band of the CLC film (not the WB CLC film) was not optimized. In addition, as mentioned above, there are some differences between the device structure of LED array and micro-LED array. Also, the insulating bank is not applied in the color-conversion film. All these factors will affect the absolute improvement of CCE by adding CLC film. However, in this proof-of-concept experiment, we

still observed that by assembling CLC films with opposite hands, the CCE of the color-conversion micro-LED display system can be improved.

5 | CONCLUSION

In this work, a patterned CLC film was proposed to enhance the CCE and color gamut of the color-converted micro-LED display. In such a display system, the thickness of p-GaN layer of blue micro-LED is optimized to achieve high LEE and small optical crosstalk. After that, a patterned CLC film with feature sizes ranging from 10 to 80 μm is fabricated. According to our simulation results, the patterned CLC film not only improves CCE by recycling the leaked blue light but also alleviates the crosstalk between green and blue CFs. Therefore, compared with a display system with CFs only, the patterned CLC film can double the CCE of display system (at 90% Rec. 2020). A proof-of-concept experiment was also conducted to verify the function of patterned CLC film. Finally, this kind of patterned CLC film is applicable to advancing all kinds of color-converted display systems.

ORCID
Ziqian He https://orcid.org/0000-0003-3560-2987
Yajie Dong https://orcid.org/0000-0001-5319-2462
Shin-Tson Wu https://orcid.org/0000-0002-0943-0440

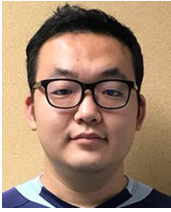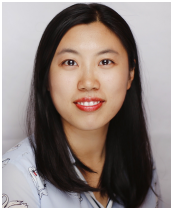## REFERENCES
1. Lin JY, Jiang HX. Development of microLED. Appl Phys Lett. 2020;116(10):100502.
2. Huang Y, Hsiang EL, Deng MY, Wu ST. Mini-LED, micro-LED and OLED displays: present status and future perspectives. Light Sci Appl. 2020;9(1):105.
3. Liu Z, Lin CH, Hyun BR, et al. Micro-light-emitting diodes with quantum dots in display technology. Light Sci Appl. 2020;9(1):83.
4. Yin Y, Hu Z, Ali MU, et al. Full-color micro-LED display with CsPbBr3 perovskite and CdSe quantum dots as color conversion layers. Adv Mater Technol. 2020;5(8):2000251.
5. Xuan T, Shi S, Wang L, Kuo HC, Xie RJ. Inkjet-printed quantum dot color conversion films for high-resolution and full-color micro light-emitting diode displays. J Phys Chem Lett. 2020;11(13):5184–5191.
6. Gou F, Hsiang EL, Tan G, Lan YF, Tsai CY, Wu ST. Tripling the optical efficiency of color-converted micro-LED displays with funnel-tube array. Crystals. 2019;9(1):39.
7. Chen GS, Wei BY, Lee CT, Lee HY. Monolithic red/green/blue micro-LEDs with HBR and DBR structures. IEEE Photonics Technol Lett. 2017;30(3):262–265.
8. Han HV, Lin HY, Lin CC, et al. Resonant-enhanced full-color emission of quantum-dot-based micro LED display technology. Opt Express. 2015;23(25):32504–32515.
9. Pan S, Duan M, Hu Z, Li D, Chen SJ, Zhang X. 86-4: color conversion enhancement of perovskite quantum dots by integrating with cholesteric liquid crystals. SID Symp Dig Tech Pap. 2020;51(1):1307–1309.
10. He J, Chen H, Chen H, Wang Y, Wu ST, Dong Y. Hybrid downconverters with green perovskite-polymer composite films for wide color gamut displays. Opt Express. 2017;25(11):2915–12925.
11. Chu SY, Wang HY, Lee CT, et al. Improved color purity of monolithic full color micro-LEDs using distributed Bragg reflector and blue light absorption material. Coatings. 2020;10(5):436.
12. Chen SWH, Huang YM, Singh KJ, et al. Full-color micro-LED display with high color stability using semipolar (20-21) InGaN LEDs and quantum-dot photoresist. Photonics Res. 2020;8(5):630–636.
13. He J, He Z, Towers A, et al. Ligand assisted swelling–deswelling microencapsulation (LASDM) for stable, color tunable perovskite–polymer composites. Nanoscale Adv. 2020;2(5):2034–2043.
14. Lien JY, Chen CJ, Chiang RK, Wang SL. 39-3: patternable color-conversion films based on thick-shell quantum dots. SID Symp Dig Tech Pap. 2017;48(1):558–561.
15. Kim HM, Ryu M, Cha JH, Kim HS, Jeong T, Jang J. Ten micrometer pixel, quantum dots color conversion layer for high resolution and full color active matrix micro-LED display. J Soc Inf Display. 2019;27(6):347–353.
16. Huang Y, Wu TX, Wu ST. Simulations of liquid-crystal Fabry–Perot etalons by an improved 4 × 4 matrix method. J Appl Phys. 2003;93(5):2490–2495.
17. Krames MR, Shchekin OB, Mueller-Mach R, et al. Status and future of high-power light-emitting diodes for solid-state lighting. J Disp Tech. 2007;3(2):160–175.
18. Zhao P, Zhao H. Analysis of light extraction efficiency enhancement for thin-film-flip-chip InGaN quantum wells light-emitting diodes with GaN micro-domes. Opt Express. 2012;20(105):A765–76.
19. Chen X, Ji C, Xiang Y, Kang X, Shen B, Yu T. Angular distribution of polarized light and its effect on light extraction efficiency in AlGaN deep-ultraviolet light-emitting diodes. Opt Express. 2016;24(10):A935–42.
20. Shen YC, Wierer JJ, Krames MR, et al. Optical cavity effects in InGaN/GaN quantum-well-heterostructure flip-chip light-emitting diodes. Appl Phys Lett. 2003;82(14):2221–2223.
21. Hu Z, Yin Y, Ali MU, et al. Inkjet printed uniform quantum dots as color conversion layers for full-color OLED displays. Nanoscale. 2020;12(3):2103–2110.
22. Yue S. P-12.4: quantum dot photoresist for color filter application. SID Symp Dig Tech Pap. 2018;49(S1):724–726.
23. He Z, He J, Zhang C, Wu ST, Dong Y. Swelling-deswelling microencapsulation-enabled ultrastable perovskite–polymer composites for photonic applications. Chem Rec. 2020;20(7):672–681.

AUTHOR BIOGRAPHIES

En-Lin Hsiang received his BS and MS degrees from National Chiao Tung University, Hsinchu, Taiwan, in 2014 and 2016, respectively. Currently, he is working toward the PhD degree at College of Optics and Photonics, University of Central Florida, USA. His current research focuses on micro-LED and mini-LED displays.

Yannanqi Li received her BS degree in Optics from Sichuan University in 2018 and is currently working toward a PhD degree at the College of Optics and Photonics, University of Central Florida. Her current research interests include novel liquid crystal optical elements, display system design, and new liquid crystal materials.

Ziqian He received his BS degree in Materials Physics from Nanjing University in 2016 and is currently working toward a PhD degree from the College of Optics and Photonics, University of Central Florida. His current research interests include liquid crystal photonics, mini-LED LCDs, micro-LED displays, and near-eye displays.

Tao Zhan received his BS degree in Physics from Nanjing University in 2016 and is currently working toward a PhD degree from the College of Optics and Photonics, University of Central Florida. His current research interests include near-eye display, planar optics, and diffractive optics.

Caicai Zhang is a doctoral student in Materials Science and Engineering at the University of Central Florida. Her research focuses on metal halide perovskite luminescent materials and devices for display, lighting, and other applications.

Yi-Fen Lan received his PhD degree from National Taiwan University in 2010. Currently, he is a principal engineer at AU Optronics Corporation. His research interests include high-dynamic-range LCDs and micro-LED displays.

Yajie Dong, Ph.D., is an associate professor at the Department of Materials Science and Engineering and NanoScience Technology Center of the University of Central Florida. He holds a joint appointment with the College of Optics and Photonics. His research focuses on luminescent nanomaterials and devices for display, lighting, photomedicine, and other applications.

Shin-Tson Wu is a Pegasus Professor at the College of Optics and Photonics, University of Central Florida. He is among the first six inductees of the Florida Inventors Hall of Fame (2014) and a Charter Fellow of the National Academy of Inventors (2012). He is a Fellow of the IEEE, OSA, SID, and SPIE and an honorary professor at Nanjing University (2013) and at National Chiao Tung University (2018). He is the recipient of 2014 OSA Esther Hoffman Beller Medal, 2011 SID Slottow-Owaki Prize, 2010 OSA Joseph Fraunhofer Award, 2008 SPIE G. G. Stokes Award, and 2008 SID Jan Rajchman Prize.